

Accepted Manuscript

Method to reduce the formation of crystallites in ZnO nanorod thin-films grown via ultra-fast microwave heating

R.J. Gray, Ayoub H. Jaafar, E. Verrelli, N.T. Kemp



PII: S0040-6090(18)30500-5
DOI: [doi:10.1016/j.tsf.2018.07.034](https://doi.org/10.1016/j.tsf.2018.07.034)
Reference: TSF 36791
To appear in: *Thin Solid Films*
Received date: 5 December 2017
Revised date: 23 May 2018
Accepted date: 25 July 2018

Please cite this article as: R.J. Gray, Ayoub H. Jaafar, E. Verrelli, N.T. Kemp , Method to reduce the formation of crystallites in ZnO nanorod thin-films grown via ultra-fast microwave heating. Tsf (2018), doi:[10.1016/j.tsf.2018.07.034](https://doi.org/10.1016/j.tsf.2018.07.034)

This is a PDF file of an unedited manuscript that has been accepted for publication. As a service to our customers we are providing this early version of the manuscript. The manuscript will undergo copyediting, typesetting, and review of the resulting proof before it is published in its final form. Please note that during the production process errors may be discovered which could affect the content, and all legal disclaimers that apply to the journal pertain.

© 2018. This manuscript version is made available under the CC-BY-NC-ND 4.0 license <http://creativecommons.org/licenses/by-nc-nd/4.0/>

Method to reduce the formation of crystallites in ZnO nanorod thin-films grown via ultra-fast microwave heating

R. J. Gray^a, Ayoub. H. Jaafar^{a,b}, E. Verrelli^a, N. T. Kemp^{a,*}

^a School of Mathematics and Physical Sciences, University of Hull, Hull, HU6 7RX, UK

^b Physics Department, College of Science, University of Baghdad, Baghdad, Iraq

* Author to whom correspondence should be addressed. Electronic mail:

N.Kemp@hull.ac.uk

Key Words: Zinc oxide, nanorods, thin-films, memristors, nucleation, crystallites, semiconductor, hydrothermal growth

Abstract

This paper discusses the nucleation and growth mechanisms of ZnO nanorod thin-films and larger sized crystallites that form within the solution and on surfaces during an ultra-fast microwave heating growth process. In particular, the work focusses on the elimination of crystallites as this is necessary to improve thin-film uniformity and to prevent electrical short circuits between electrodes in device applications. High microwave power during the early stages of ZnO deposition was found to be a key factor in the formation of unwanted crystallites on substrate surfaces. Once formed, the crystallites, grow at a much faster rate than the nanorods and quickly dominate the thin-film structure. A new two-step microwave heating method was developed that eliminates the onset of crystallite formation, allowing the deposition of large-area nanorod thin-films that are free from crystallites. A dissolution-recrystallization mechanism is proposed to explain why this procedure is successful and we demonstrate the importance of the work in the fabrication of low-cost memristor devices.

Introduction

Zinc oxide (ZnO) is a semiconductor with a wide direct band gap energy of ~ 3.4 eV and a large exciton binding energy of 60 meV at 300 K [1], [2]. It has gained increasing interest in

recent years due to its applications in solar cells [3]–[8], thin film transistors [3]–[5], [9], [10], resistive switching memory devices [11]–[14] and transparent conductive oxides [15]–[19]. It is an inexpensive material that can be processed through a variety of techniques, creating a range of different nanoscale structures including nanoparticles (0-D structures), nanorods and nanorods (1-D structures), and nano thin-films (2-D structures) [20].

ZnO nanorods are of particular interest due to the ease of synthesis. Popular methods include gas-phase, or vapour-phase, synthesis (including vapour-solid and vapour-liquid-solid deposition methods) and solution-phase synthesis (including hydrothermal methods)[21]. Gas-phase synthesis methods are typically carried out at high temperatures (500°C - 1500°C) and is used to produce high aspect ratio nanorods with a highly crystalline structure, but such high temperatures are unsuitable for many processes due to thermal constraints on the substrate or other materials in the device. Solution-phase synthesis allows nanorods to be synthesized at much lower temperature (<200°C) and has as well advantages of low cost, high scalability and easier setup [20]. However, hydrothermal growth methods are often associated with long growth times, typically 10 hours or greater for high-quality nanowire growth using conventional hot-plate methods [4,7,21,23]. Recently, microwave heating has been shown to drastically reduce the growth duration to minutes whilst maintaining good film morphology and ZnO crystallinity[22][24][25].

Recently we have used a rapid microwave-assisted synthesis method to make memristor devices that are simple to produce and low cost whilst still retaining good resistance switching properties[24]. However, device yield was initially poor because many of the devices suffered from the formation of large crystallites in the nanorod thin-films, which affects the electronic switching properties of the device by modifying the interface between the electrode and the switching materials or worse, producing direct short-circuits between the device electrodes. In this paper, we report on a new approach that consistently provides nanorod thin-films that are free from crystallites. Our work demonstrates the importance of high controlled growth in the early stages of ZnO nanorod formation, which is also generally applicable to other hydrothermal growth methods that also suffer from the formation of large crystallites [21]. We demonstrate the importance of controlled temperature and pressure throughout the growth process and almost complete elimination

of the crystallites via a two-step microwave growth method involving first an initial stage of slow growth followed by a stage of faster growth.

Experimental Method

The microwave synthesis method was adapted from previously published methods (3,21,22). Prior to microwave synthesis, 25 mm x 25 mm ITO-coated float glass substrates were cleaned by ultrasonication in acetone and propan-1-ol respectively for 5 minutes in each solvent, followed by repeated rinsing with deionized water (16 M Ω) and drying with nitrogen gas. A seed layer was first deposited on the substrates by spincoating a 10 mM solution of zinc acetate dihydrate (99%, Sigma-Aldrich) in propan-1-ol at 2000 rpm for 30 seconds. This was followed by annealing on a hot plate at 300°C for 30 minutes to align the crystalline structure of the seeds so that vertical nanorods grow. The spin coating and annealing steps are repeated 3 times.

Growth of nanorods from the seed layer was carried out by microwave heating of the submerged substrate in a 25 mM (equimolar) solution of zinc nitrate hexahydrate (99%, Sigma-Aldrich) and hexamethylene tetramine (99.5%, Sigma-Aldrich) dissolved in deionized water. Initial experiments used a conventional microwave oven with samples submerged vertically in a crystallizing dish containing 50 ml of the growth solution and with heating for 2 minutes in a 900 W Russell Hobbs domestic microwave (25 L Convection Microwave Oven, Model Number RHM2507); the method was refined by using a MARS 5 (CEM) scientific microwave with temperature ($\pm 1^\circ\text{C}$) and pressure control. Samples were submerged vertically in 25 ml vials that are sealed with caps to prevent evaporation of the solution and provide control of the pressure. A temperature probe was placed in one of the vials for temperature control and the microwave was set to maintain a pressure < 50 PSI during growth of the nanorods. During growth of the nanorods the pressure was observed to never rise above 15 PSI whilst the typical pressure build-up was ~ 5 PSI. A two-step method was developed to initially grow a uniform layer of nanoscale nodules (ramp phase) from which the nanorods could be extended to longer lengths (growth phase) without the deposition of crystallites. The diameters of the nanorods were typically 40-50 nm but the nanorod length is dependent on the growth time and heating method. High quality thin films of long nanorods (600 nm) could easily be grown using the two-step method but this was not the case with the other methods since once the crystallites form their growth

dominates and can in some cases completely cover the nanorod layer. Films grown using the two-step method had a high degree of uniformity across the substrate (i.e. nanorods had equal length and diameter). The RMS roughness of these film were ~ 6.9 nm (Bruker AFM). In contrast the RMS roughness of the seed layer was 1.47 nm.

Memristor devices were made using the following procedure. ITO coated substrates were cleaned by rinsing in DI water, dried under nitrogen flow and then coated with a ZnO nanorod thin-film using the above seeding process and two-step microwave heating method to give ~ 50 nm diameter nanorods with length ~ 400 nm. Afterwards, a polymer layer was spin-coated on the device using a PMMA solution (Sigma Aldrich, 120,000 M_w , 3% by weight in toluene) at 2000 rpm for 60 s, followed by annealing at 150°C for 30 minutes to remove any remaining solvent. This typically resulted in a PMMA thickness of ~ 50 -100 nm with a RMS roughness of 6.79 nm, which is slightly smaller than the nanorod thin-film, possibly due to the tendency of the PMMA to fill in the gaps between the nanorods. Top contacts of the devices consisted of either Al (100 nm thick) or Au, deposited by thermal evaporation under vacuum conditions through a mask containing 100, 200 and 400 μm diameter circles. I-V characteristics and pulse measurements were carried out using a probe station equipped with an HP4140B source-meter unit. All measurements were carried out at room temperature in ambient atmosphere.

Results

Figure 1 shows typical SEM images of samples produced using the initial method for microwave-assisted nanorod growth using a domestic microwave. While the method produced a uniform thin-film of vertically oriented nanorods all having the same diameter and length, it was clear that larger crystallites also formed at the same time. These crystallites were of sizes exceeding 1 μm and often appeared in clusters that were ~ 10 μm in size. The formation of the crystallites was not easily controllable or predictable; some samples exhibited few crystallite clusters, while other samples were dominated by crystallite structures throughout the entire surface of the substrate.

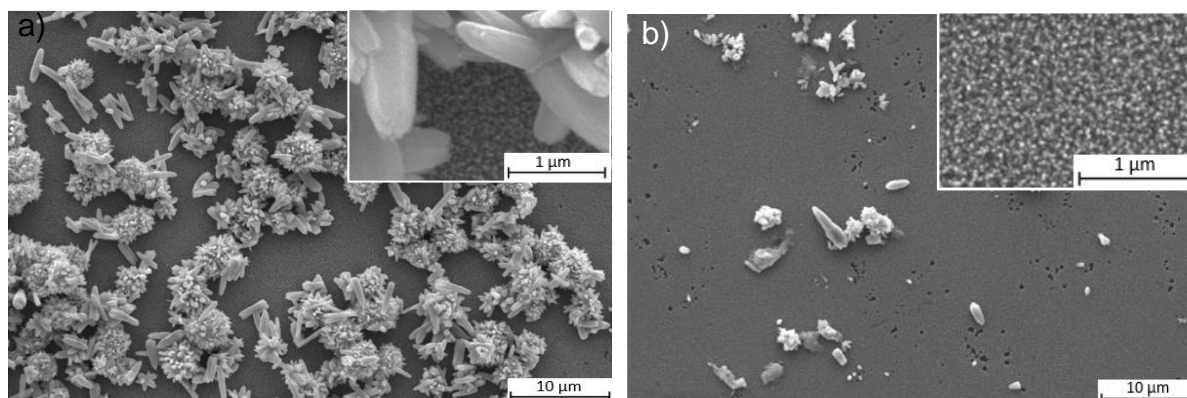


Fig. 1: SEM images showing nanorods and crystallites on glass substrates using our initial domestic microwave approach with a 5 minute growth period. Crystallites are significantly larger than the nanorods and typically appear throughout the substrate surface, although the density of crystallite clusters varies from one sample to another. The inset of a) shows the crystallites more clearly with the nanorods in the background.

To address the problem of the formation of large crystallites, a new two-step microwave heating method was developed consisting of first a slow ramp to the growth temperature, to form small nanoscale nodules from the seeds, followed by a second step that maintained the desired temperature (80°C) and grew the nanorods outwards from the small nodules. To achieve this a scientific grade microwave was used that had both temperature and pressure control. Figure 2 show SEM images of ZnO thin-films grown using the two-step heating method but with different high and low power ramp stages. Figure 2a consisted of a fast ramp to 80°C (over 5 minutes) using 1600 W heating, followed by a 20 min growth period at 80°C. In contrast, Figure 2b, used a much lower power (100 W) and a longer initial growth step (15 min) before heating at 80°C for 20 minutes to grow the nanorods. This sample shows almost no large crystallite formation, whereas in contrast the sample heated at high power shows inhomogeneous growth (darkened regions) and a much greater concentration of large crystallites.

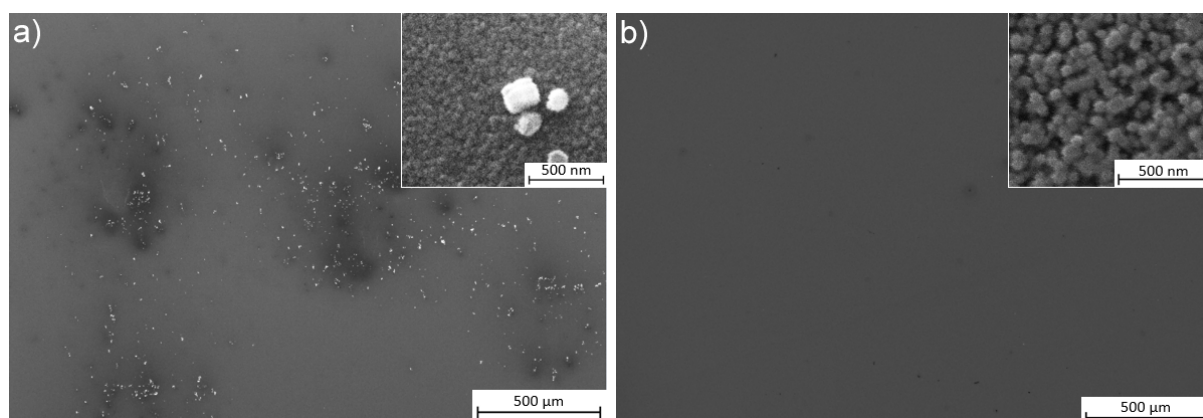


Fig. 2: SEM images showing nanorods and crystallites formed on glass substrates using the scientific grade microwave approach with heating a) at 1600 W power for a ramp duration of 5 minutes before holding at 80°C for 20 minutes and b) at 100 W power for a ramp duration of 15 minutes before holding at 80°C for 20 minutes. The reduction in microwave power during the initial stage of growth significantly reduces the number of crystallites on the substrate surface. The insets at higher magnification show the nanorods and crystallites much more clearly.

The two methods of controlled heating (100 W and 1600 W) using the scientific grade microwave were further compared by varying the “hold” duration (the duration for which the sample is maintained at 80°C). Once the desired temperature was reached, the temperature was maintained for 5, 10, 20 and 30 minutes. Figure 3 shows the graph of the average number of crystallites per device measured on four samples grown at 1600 W and four grown at 100 W. Since each device electrode was a circle with a diameter of 200 μm, 1 defect per device is equivalent to 1 defect per $31 \times 10^{-3} \text{ mm}^2$ (or ≈ 32 defects per mm^2). A minimum crystallite size of 200 nm was used in the counting process. This was chosen because the growth of crystallites is faster than that of the nanorods and if a crystallite forms it typically grows to at least this size. From the graph it can be seen that the low-power ramp-to-temperature step has substantially fewer crystallites in the same area even though some samples were grown with long heating times. No study was undertaken on the dependence of the size of crystallites, as the focus of this work was rather their elimination, it was generally observed however that once crystallites form, higher growth temperatures gave faster growth and therefore larger crystallites. Larger heating rates were also examined but were not included in the study because the crystallites join together, making their counting (as individuals) difficult.

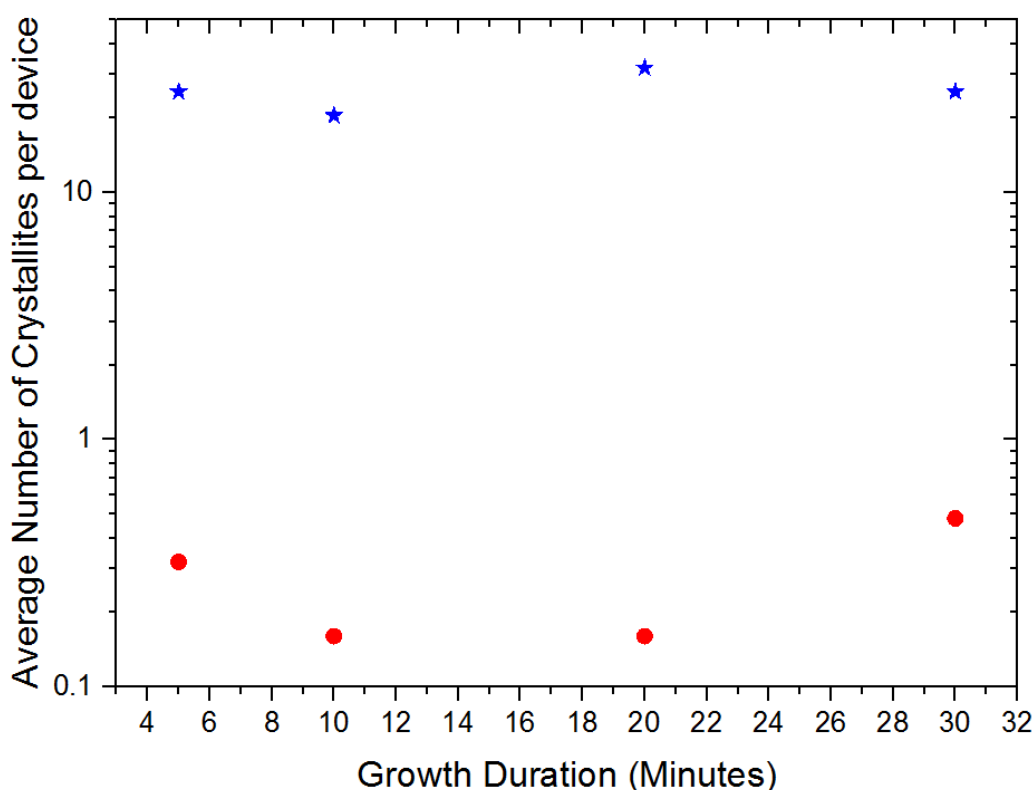


Fig. 3: A graph of the average number of crystallites per device for samples grown at high (● 1600 W) and low (★ 100 W) microwave power (note: the area of each device is $31 \times 10^{-3} \text{ mm}^2$). The duration of the ramp to the growth temperature (80°C) was 5 minutes for the 1600 W samples and 15 minutes at 100 W. After the ramp stage the samples were then held at 80°C for 5, 10, 20 and 30 minutes. As can be seen in the graph the number of crystallites formed is independent of the growth duration indicating that crystallite formation occurs only in the very early stages of growth.

The graph in figure 4 shows the temperature profile of the scientific grade microwave throughout the growth step, both at 100 W and 1600 W power, compared against a domestic microwave at 900 W. The temperature control of the scientific grade microwave ensures that the ramping stage is very close to linear, slightly adjusting the power input to ensure steady, constant heating to temperature. These slight power adjustments are responsible for the slight loss of linearity for the final point on each respective line. The domestic microwave lacks this fine-tuning capability, and so the ramping stage is less linear and more prone to overshooting the desired temperature. This was partially

corrected, albeit in only a limited manner, as it is highly specific to the temperature and rate of temperature change, by using a water bath approach. This consisted of placing a large water bath (1250 mL) inside the microwave and positioned around the sample beaker. In this way the temperature profile of the scientific grade microwave could be reproduced as shown by the similarity of the blue and black lines in Figure 4. In this case, although the heating rate of the water bath method was similar to the 100 W commercial microwave method the number of crystallites observed was still slightly less in the commercial microwave. As yet, we cannot attribute this to any particular cause, although lack of control of the pressure may be a possibility.

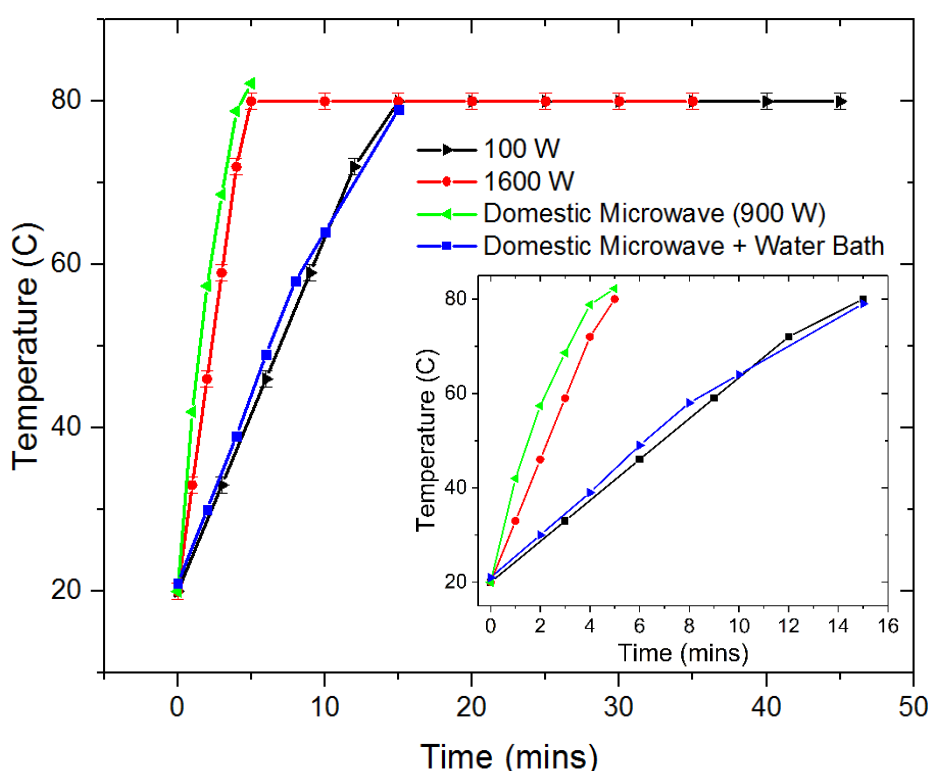


Fig. 4: Temperature profiles of the different heating methods used for growth of the ZnO nanorods. The methods consisted of a scientific grade microwave with heating at 100 W (black data) and 1600 W (red data), and a domestic microwave with (blue data) and without (green data) a water bath. The inset shows an enlarged view of the temperature profiles during only the ramping step.

To determine the point at which crystallites form on the substrate we performed a growth study that involved SEM imaging of the samples at specific times (20 s, 40 s and 60 s) during deposition of the nanorods. For this procedure the domestic microwave oven at a

100% power setting (900 W) was used. All samples were heated in the growth solution in the centre of the microwave, revolving at 6 rotations per minute. The SEM results are shown in figure 5 below. Except for the sample with just the seed layer, figure 5a), the early stages of crystallite growth are visible on all of the SEM images, appearing as large white “dots” on the samples’ surfaces. Due to the small time each sample spends in the growth solution, there is little to no nanowire growth. Early signs of nanowire growth are only obvious in figures 5c and 5d is because the solution only exceeds the minimum ideal growth temperature for nanorod growth ($\sim 70^{\circ}\text{C}$) at around 40 s in the commercial microwave (the 20 s sample reached only $\sim 40^{\circ}\text{C}$).

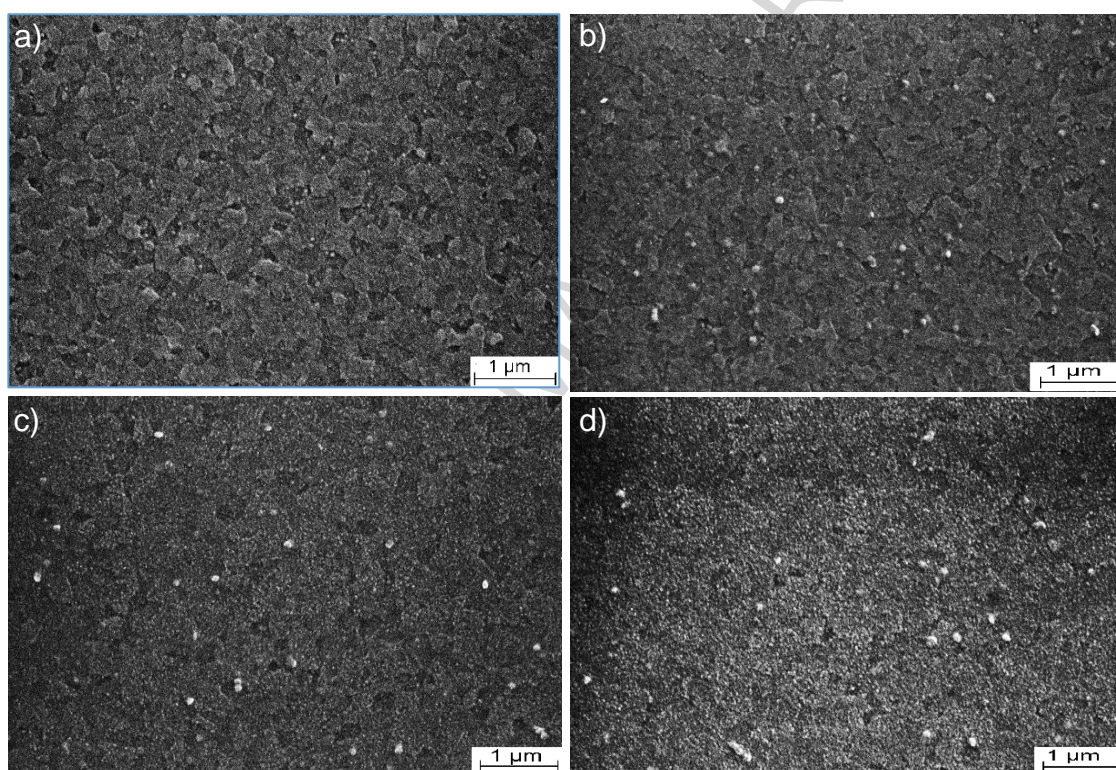


Fig. 5: SEM images of a) a control sample that has received a seed layer and has been dipped into the growth solution for one minute, and samples containing seed layers that were heated in a commercial microwave at 100% power for b) 20 s, c) 40 s and d) 60 s. In each case the ITO is clearly visible whilst images in c) and d) show the very early stages of nanowire growth. Early stages of crystallite growth also appear as white protrusions.

To investigate further the early stages of nucleation and growth of the nanorods and crystallites, an atomic force microscope (AFM) study was undertaken on samples grown at high heating rates with the 1600 W scientific grade microwave. Silicon substrates were

used in this case, as these are very flat and are better for AFM imaging purposes. No differences were observed between growth on different substrates (ITO, glass or Si) and in other work (not shown here) we have also observed no differences growing the nanorods on common metals (e.g. gold), which indicates the surface material does not play a role in the growth process. Initially, just the seed layer was investigated to determine if defects in this layer could be identified as a starting point of crystalline growth. We found no evidence of this and instead focussed on identifying the starting point of crystallite formation during the nanorod growth. Figure 6 shows AFM images of growth on seeded Si substrates with growth times of 20 s, 40 s and 60 s. The AFM images indicate the uniform deposition of small nucleation centres (at 20 s) that extend outward as they grow to form the beginning of the nanorods (at 60 s). Interestingly, crystallites were found on all of these samples (although images of them are not shown because their size affected the AFM scan and distorted the images). This indicates that crystallites form directly at the onset of nanorod growth if high heating rates are used from the beginning. In contrast, when the two-step 100 W ramped method was used, as discussed in Fig.3, crystallite formation was rare.

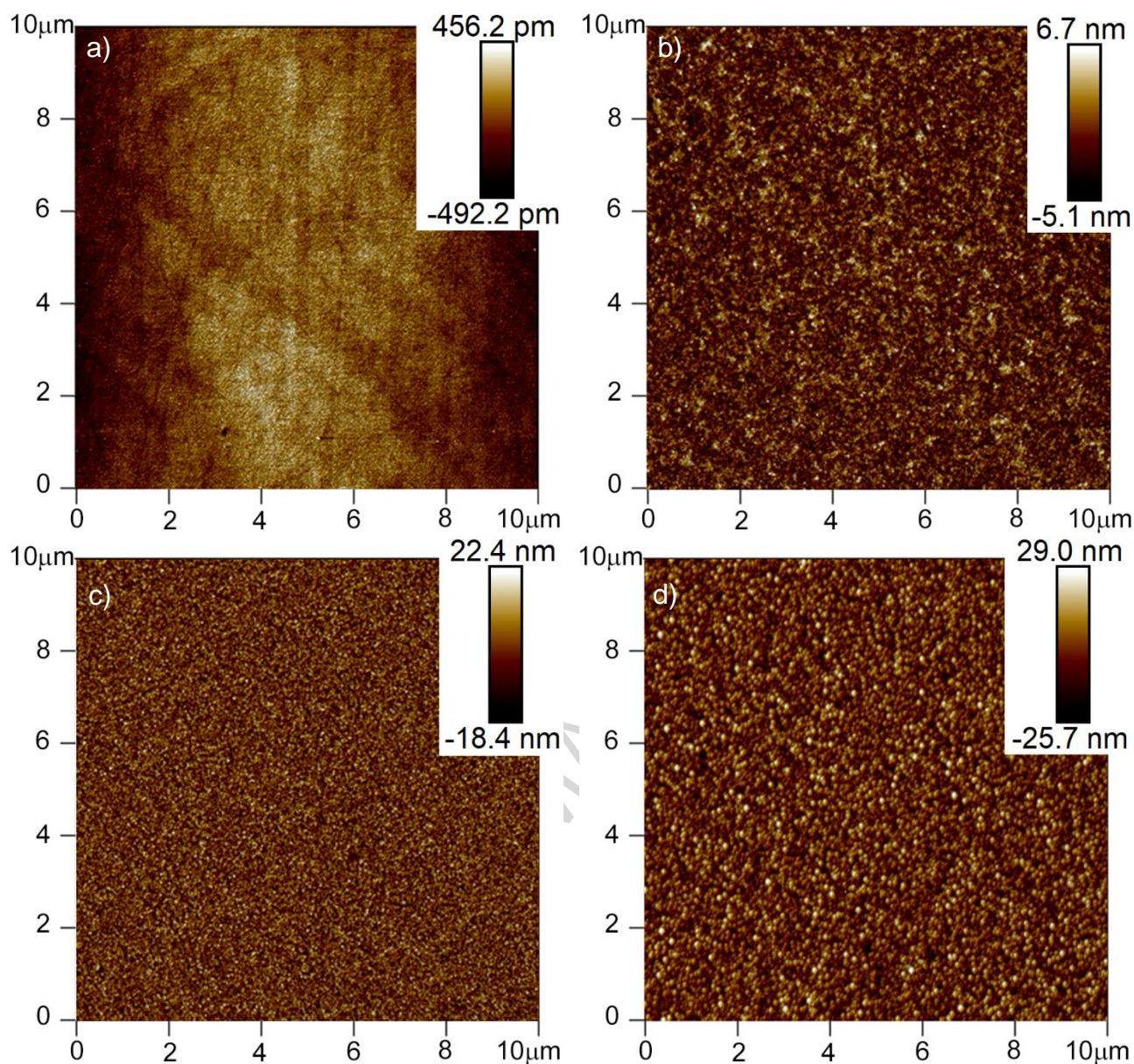


Fig. 6: AFM images showing the early stages of nanorod growth on Si substrates using the high power (1600 W) scientific grade microwave method and with heating times of b) 20 s, c) 40 s and d) 60 s. For comparison a control sample showing a smooth bare substrate is shown in a). Crystallites were found to be present in b), c) and d), however these are not shown as the AFM image becomes distorted when large crystallites are encountered.

The importance of depositing crystallite free ZnO nanorod thin films for memristor device applications is demonstrated in Figure 7. The device structure, Figure 7a, consists of an indium tin oxide (ITO) coated glass substrate as a common bottom electrode followed by a thin-film of aligned ZnO nanorods, grown using the microwave heating method, a spin-

coated PMMA layer and finally, top electrodes made from thermally evaporated Aluminium. A picture of the final device is shown in Figure 7b.

A comparison of the typical memristor switching properties of devices with and without crystallites is shown in the current-voltage sweeps in Figure 7c and 7d respectively. Normal memristor behaviour is synonymous with a pinched hysteresis current-voltage curve (pinched at the origin) having high and low current paths that represent the on and off resistive states of the device, respectively. To better depict symmetrical aspects between the two sides of the pinched hysteresis it is common practice to plot the absolute current density (J) on a log axis versus the electric field on a linear axis. The red and black curves represent the on and off states of the device respectively. Figure 7c shows the typical current-voltage characteristics of a device containing a large number of crystallites. Since this device contains large crystallites that short-circuit through the PMMA layer the device current is large and reaches current compliance at a low voltage (as indicated by the flat line). Large device currents are undesirable in memory technologies because of their high power usage. The device in Figure 7c also exhibits poor switching properties, including unpredictable changes in current during a single I–V sweep and erratic changes in the set and reset voltages. In some sweeps (as shown) the device exhibits switching at a potential with polarity that is opposite to what is expected (i.e. negative voltage instead of positive as shown at $E=-0.01$ MV/cm), which indicates poor device stability. In contrast, Figure 7d shows the current-voltage switching properties of device containing no crystallites. In this case there is a clear and consistent separation between states and the device exhibits reliable and repeatable switching characteristics with a lower device current.

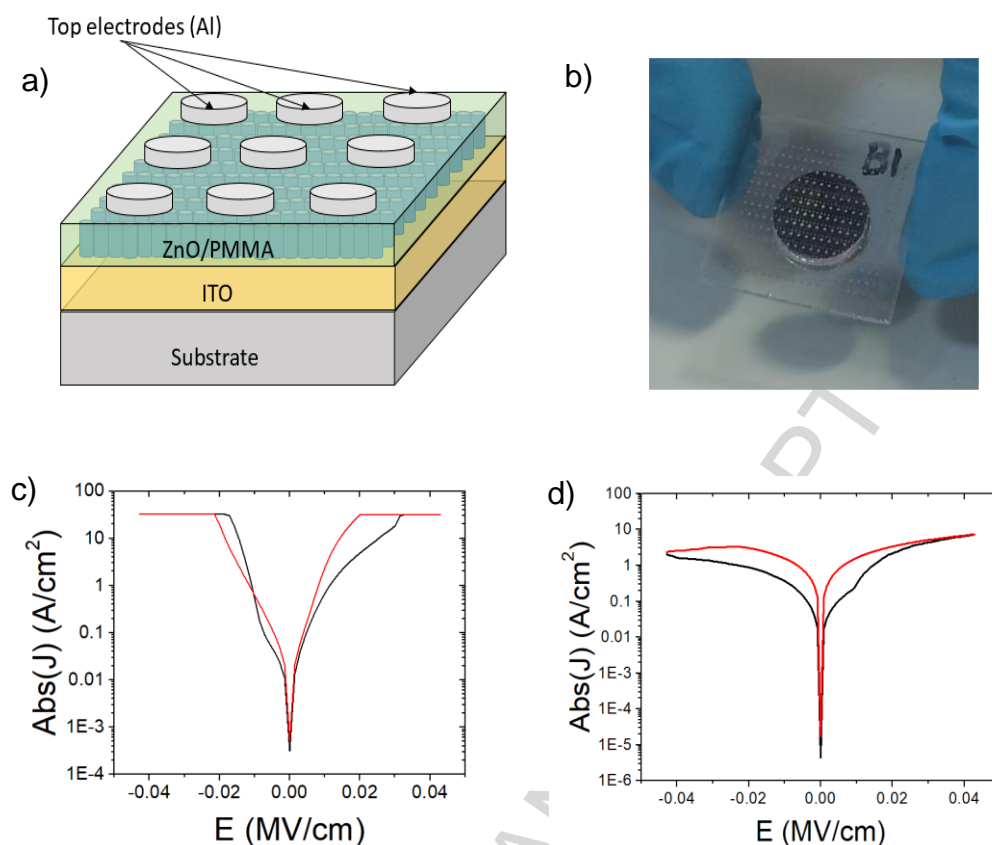


Fig. 7: a) The schematic of a ZnO nanorod-PMMA hybrid memristor device consisting of a common ITO bottom electrode and individual Al top electrodes for each device. b) A photograph of a completed sample of many memristor devices, produced using our growth method. (Note: the dark patch underneath the device is an SEM stub) c) A plot of absolute current density vs. electric field for a memristor device containing many large crystallites and resulting in inconsistent and unreliable memristor switching properties. d) A plot of absolute current density vs. electric field for a typical memristor containing no crystallites and exhibiting repeatable and reliable memristor switching properties.

Discussion

ZnO is formed in the growth step by a series of chemical reactions, and the rate at which these chemical reactions occur is key to controlling the formation and deposition of large crystallites as opposed to the desired nanowire structures. The reaction steps are as follows [20]:

- Decomposition reaction:



- Hydroxyl supply reaction:



- Supersaturation reaction:



- ZnO nanowire growth reaction:



The HMTA in the solution serves three main roles: it provides the OH^- ions needed to initiate the hydroxyl reaction; it acts as a pH buffer within the solution, as the hydrolysis rate of HMTA is decreased by an increase in pH and vice versa; it also attaches to the non-polar facets of the nanorods during growth, preventing the access of Zn^{2+} ions to these facets and thereby leaving only the polar (001) face for epitaxial growth [20], [26].

It is believed that high supersaturation levels favour nucleation while low supersaturation levels favour crystal growth [20], [27], and as such the second of the roles listed above is particularly key. Rapid production of OH^- ions within a short period causes Zn^{2+} ions to precipitate out quickly due to the high pH environment, minimizing the contribution of the Zn^{2+} ions to the nanowire growth and rapidly consuming the nutrient, resulting in the eventual prohibition of further growth of the nanorods [28]. The use of HMTA in the growth solution contributes to maintaining a low supersaturation level by controlling the concentration of OH^- ions in the solution. It is this characteristic behaviour that appears to govern the formation and deposition of the large crystallites. It is observed that neither crystallites nor nanorods grow at very low temperatures; as shown by the SEM images in figure 5, along with the heating profile data from figure 4, the crystallites and nanorods only begin to form once the temperature reaches $\sim 70^\circ\text{C}$. However, rapid temperature ramping at high power causes significantly more crystallites to be formed on substrates than slow ramping at much lower power, keeping the post-ramping duration the same in each case. These results can be observed in figures 1 and 2a above, compared with figure 2b, as both the domestic microwave and 1600 W heating methods have a fast rate of temperature increase compared with the 100 W heating method. By counting the number

of crystallites in a well-defined region it is shown, Figure 3, that there is a large reduction ($\approx 90\%$) in the formation of crystallites using low power heating and a longer ramp duration.

In 2007 it was demonstrated [29] that growth of nanocrystals and crystallites in the presence of a capping agent occurs at a much slower rate than the generally accepted mechanism of Ostwald ripening, which is a diffusion limited process occurring in the last stage of a first-order phase transformation; Alikakos et al (2004) tell us that:

“Usually, any first-order phase transformation process would result in a two-phase mixture with a dispersed second phase in a matrix. Initially, the average size of the dispersed particles is very small and therefore the interfacial energy of the system is large and the mixture is not in equilibrium” [30].

The Gibbs-Thomson condition explains that the gradient of the chemical potential on the interface is proportional to its mean curvature. As such, matter from small particles (regions of higher curvature) diffuses to larger particles (regions of lower curvature), ultimately resulting in the smaller particles shrinking to nothing while larger particles grow in size [30].

However, as explained in [29], the presence of a capping agent slows down Ostwald ripening. In this case, HMTA acts as a capping agent, particularly limiting growth in the non-polar directions but also helping to prevent the formation of larger crystallites on the sample surface. In spite of this, quick ramping to temperature in a microwave still yields large crystallites across the substrate surface; slower ramping, however, produces much less crystallites. Further, heating by using high-power microwave pulses to artificially generate the same ramp duration for heating to 80°C as used for the low-power ramp method, still produces large crystallites; on the other hand, submerging a vial containing the growth solution and substrate into a larger water bath in the domestic microwave allows a more natural fit to the ramping rate produced by the 100 W method, producing less large crystallites than the quick ramp method. It is therefore proposed that the intensity of the microwave radiation during heating plays a crucial role in the formation of crystallites, with a faster rate of temperature increase in the solution overwhelming the capping effects of the HMTA and encouraging Ostwald ripening.

Although rapid, high power heating may cause more crystallites to form on the substrates, both the 1600 W and 100 W heating methods produce a cloudy, “milky” white solution by the time the deposition process is completed. This is caused by ZnO particles precipitating out in the solution, which happens extremely slowly in ambient conditions at room temperature but happens quickly when heated to 80°C.

As can be seen in figures 1 and 2a, large crystallites appear to rest on top of the nanorod films when heated rapidly; this would indicate that the crystallites form in the solution itself and “settle” onto the substrate. However, the large crystallites are not all removed after rinsing with deionized water and drying with pressurised nitrogen gas. In addition, the crystallites also appear on the “top” face, even when the “top” face of the substrate is facing down into the solution; this makes “settling” due to gravity unlikely. Instead we propose, and as figure 5 suggests, that crystallites form directly onto the substrate during the early stages of heating and undergo rapid growth via an Ostwald-like ripening process to form the larger crystallite structures seen in figure 1.

Our studies therefore show that in general, the route to reducing the formation of large crystallites requires the deposition of a uniform seed layer, a steady and low-rate ramp to the growth temperature, and good temperature and pressure control. The alignment, crystallinity and size of the seeds is an important starting point as it governs the resulting alignment of the nanorods, their diameter and overall film morphology of the nanorod thin-film. [20][27][31][32] Here The highly controlled growth in the very early stages of growth, i.e. the formation of the nanorod nodules, is critical for eliminating crystallite formation and growth. A similar process has been established by us previously for the growth of conducting polymer nanowires [33][34], where we showed the importance of stepwise nucleation and growth mechanisms in promoting nanowire growth whilst eliminating the formation and growth of larger polymer fibrils during the nanowire elongation process.

In summary, hydrothermal methods for growing ZnO nanorods are typically associated with long growth times (10 hours or more) and can still have significant defects present in the thin-films (4,7,21,). Recently, microwave heating has been shown to drastically reduce the growth duration of ZnO nanorods to minutes[22] and in this work we have shown how slightly longer growth times using a two-step microwave growth process can greatly

improve the quality of films (by eliminating the formation of crystallites) but without significantly sacrificing the deposition time. The realization of fast depositions method is a significant advantage in the large scale production of electronic devices and recently we have used this technique to fabricate a number of ZnO based electronic and optoelectronic memristor devices[24][25]. Figure 7 demonstrates the importance of having high-quality nanorod thin-film growth for memory devices, since large crystallites affect the devices switching properties and/or creates high-current short-circuit pathways.

Conclusion

It has been shown that the rate of temperature change of the growth solution greatly affects crystallite formation when depositing ZnO nanorods thin-films. A correlation exists between the initial rate of microwave heating (to reach the desired temperature) and the number of crystallites formed. Using a scientific grade microwave, a 1600 W high-rate ramp to 80°C produces significantly more large crystallites than a 100 W low-rate ramp. The number of crystallites formed does not depend on total growth duration; instead, the rate of ramping to temperature, the quality of the seed layer, and good temperature and pressure control strongly influences the growth of large crystallites on the sample surface. A new two-step microwave growth procedure was developed that eliminates the onset of crystallite formation, allowing the deposition of large-area nanorod thin-films that are free from crystallites. We demonstrate the importance of having high-quality ZnO nanorod thin-films that are free of crystallites on the electronic switching properties of memristor devices.

Acknowledgments

We would like to sincerely thank support from the Iraqi Ministry of Higher Education and Scientific Research (University of Baghdad) for partial funding of this work and help with SEM imaging from Garry Robinson (School of Engineering, University of Hull). The authors would like to acknowledge the contribution of the COST Action IC1401.

References:

- [1] F. Lu, W. Cai, and Y. Zhang, "ZnO Hierarchical Micro / Nanoarchitectures : Solvothermal Synthesis and Structurally Enhanced Photocatalytic Performance *," *Adv. Funct. Mater.*, vol. 18, no. 7, pp. 1047–1056, 2008.
- [2] T. A. Krajewski, G. Luka, L. Wachnicki, R. Jakiela, B. Witkowski, E. Guziewicz, M. Godlewski, N. Huby, and G. Tallarida, "Optical and electrical characterization of defects in zinc oxide thin films grown by atomic layer deposition," *Opt. Appl.*, vol. 39, no. 4, pp. 865–874, 2009.
- [3] L. E. Greene, B. D. Yuhas, M. Law, D. Zitoun, and P. Yang, "Solution-Grown Zinc Oxide Nanowires," *Inorg.Chem.*, vol. 45, no. 19, pp. 7535–7543, 2006.
- [4] Q. Li, V. Kumar, Y. Li, H. Zhang, T. J. Marks, and R. P. H. Chang, "Fabrication of ZnO Nanorods and Nanotubes in Aqueous Solutions," *Chem. Mater.*, vol. 17, pp. 1001–1006, 2005.
- [5] G. D. Yuan, W. J. Zhang, J. S. Jie, X. Fan, J. A. Zapien, Y. H. Leung, L. B. Luo, P. F. Wang, C. S. Lee, and S. T. Lee, "p-Type ZnO Nanowire Arrays," *Nano Lett.*, vol. 8, no. 8, pp. 2591–2597, 2008.
- [6] Y. Qin, X. Wang, and Z. L. Wang, "Microfibre-nanowire hybrid structure for energy scavenging," *Nature*, vol. 451, no. 7180, pp. 809–13, 2008.
- [7] H. E. Unalan, P. Hiralal, N. Rupesinghe, S. Dalal, W. I. Milne, and G. A. J. Amaratunga, "Rapid synthesis of aligned zinc oxide nanowires.," *Nanotechnology*, vol. 19, no. 25, p. 255608, 2008.
- [8] W. G. Yang, F. R. Wan, S. W. Chen, and C. H. Jiang, "Hydrothermal Growth and Application of ZnO Nanowire Films with ZnO and TiO₂ Buffer Layers in Dye-Sensitized Solar Cells," *Nanoscale Res. Lett.*, vol. 4, no. 12, pp. 1486–1492, 2009.
- [9] Z. L. J. Cheng, X. Zhang, "Aligned ZnO nanorod arrays fabricated on Si substrate by solution deposition," *Phys. E Low-dimensional Syst. Nanostructures*, vol. 31, pp. 235–239, 2006.
- [10] P.-C. Chang and C.-J. Chien, "Finite size effect in ZnO nanowires, Applied Physics Letters," *Appl. Phys. Lett.*, vol. 90, p. 113101, 2007.
- [11] A. Kumar, Y. Rawal, and M. S. Baghini, "Fabrication and Characterization of the ZnO-based Memristor," in *2012 International Conference on Emerging Electronics (ICEE)*, 2012, pp. 1–3.

- [12] M. Lanza, "A Review on Resistive Switching in High-k Dielectrics: A Nanoscale Point of View Using Conductive Atomic Force Microscope," *Materials (Basel)*, vol. 7, pp. 2155–2182, 2014.
- [13] J. Park, S. Lee, J. Lee, K. Yong, and K. Y. J. Park, S. Lee, J. Lee, "A light incident angle switchable ZnO nanorod memristor: Reversible switching behavior between two non-volatile memory devices," *Adv. Mater.*, vol. 25, no. 44, pp. 6423–6429, 2013.
- [14] C.-H. Huang, J.-S. Huang, C.-C. Lai, H.-W. Huang, S.-J. Lin, and Y.-L. Chueh, "Manipulated transformation of filamentary and homogeneous resistive switching on ZnO thin film memristor with controllable multistate," *ACS Appl. Mater. Interfaces*, vol. 5, no. 13, pp. 6017–6023, 2013.
- [15] X. Jiang, F. L. Wong, M. K. Fung, S. T. Lee, and X. Jiang, "Aluminum-doped zinc oxide films as transparent conductive electrode for organic light-emitting devices Aluminum-doped zinc oxide films as transparent conductive electrode for organic light-emitting devices," *Appl. Phys. Lett.*, vol. 1875, no. 2003, pp. 2001–2004, 2013.
- [16] C. Bundesmann, R. Schmidt-Grund, and M. Schubert, "Optical Properties of ZnO and Related Compounds," in *Transparent Conductive Zinc Oxide: Basics and Applications in Thin Film Solar Cells*, K. Ellmer, A. Klein, and B. Rech, Eds. 2008, pp. 79–124.
- [17] K. Ellmer, "Magnetron sputtering of transparent conductive zinc oxide: relation between the sputtering parameters and the electronic properties," *J. Phys. D. Appl. Phys.*, vol. 33, no. 4, pp. R17–R32, 2000.
- [18] M. Chen, Z. L. Pei, X. Wang, C. Sun, and L. S. Wen, "Structural, electrical, and optical properties of transparent conductive oxide ZnO:Al films prepared by dc magnetron reactive sputtering," *J. Vac. Sci. Technol. A Vacuum, Surfaces, Film.*, vol. 19, no. 3, pp. 963–970, 2001.
- [19] M. K. A. Yamada, B. Sang, "Atomic layer deposition of ZnO transparent conductive oxides," *Appl. Surf. Sci.*, vol. 112, pp. 216–222, 1997.
- [20] Y. Zhang, M. K. Ram, E. K. Stefanakos, and D. Y. Goswami, "Synthesis, Characterization, and Applications of ZnO Nanowires," *J. Nanomater.*, vol. 2012, p. 624520, 2012.
- [21] A. D. Mason, T. J. Waggoner, S. W. Smith, J. F. C. Jr, B. J. Gibbons, D. T. Price, and D. D. A. Allman, "Hydrothermal Synthesis of Zinc Oxide Nanowires on Kevlar using ALD and Sputtered ZnO Seed Layers," *Mater. Res. Soc. Symp. Proc.*, vol. 1178, pp. 3–9, 2009.

- [22] A. D. Mason, T. F. Roberts, J. F. Conley, D. T. Price, D. D. J. Allman, and M. S. McGuire, "Investigation of growth parameter influence on hydrothermally grown ZnO nanowires using a research grade microwave," in *2009 International Semiconductor Device Research Symposium*, 2009, no. 3, pp. 1–2.
- [23] F. A. Alharthi, F. Cheng, E. Verrelli, N. T. Kemp, A. F. Lee, M. A. Isaacs, M. O'Neill, and S. M. Kelly, "Solution-processable, niobium-doped titanium oxide nanorods for application in low-voltage, large-area electronic devices," *J. Mater. Chem. C*, vol. 6, no. 5, pp. 1038–1047, 2018.
- [24] E. Verrelli, R. J. Gray, M. O. Neill, S. M. Kelly, and N. T. Kemp, "Microwave oven fabricated hybrid memristor devices for non-volatile memory storage," *Mater. Res. Express*, vol. 1, no. 4, p. 046305, 2014.
- [25] A. H. Jaafar, R. J. Gray, E. Verrelli, M. O'Neill, S. M. Kelly, and N. T. Kemp, "Reversible optical switching memristors with tunable STDP synaptic plasticity: a route to hierarchical control in artificial intelligent systems," *Nanoscale*, vol. 9, no. 43, p. 17091, 2017.
- [26] A. Sugunan, H. C. Warad, M. Boman, and J. Dutta, "Zinc oxide nanowires in chemical bath on seeded substrates: role of hexamine," *J. Sol-Gel Sci. Technol.*, vol. 39, no. 1, pp. 49–56, 2006.
- [27] B. Weintraub, Z. Zhou, Y. Li, and Y. Deng, "Solution synthesis of one-dimensional ZnO nanomaterials and their applications," *Nanoscale*, vol. 2, no. 9, p. 1573, 2010.
- [28] S. Xu, C. Lao, B. Weintraub, and Z. L. Wang, "Density-controlled growth of aligned ZnO nanowire arrays by seedless chemical approach on smooth surfaces," *J. Mater. Res.*, vol. 23, no. 08, pp. 2072–2077, 2008.
- [29] R. Viswanatha, H. Amenitsch, and D. D. Sarma, "Growth Kinetics of ZnO Nanocrystals: A Few Surprises," *J. Am. Chem. Soc.*, vol. 129, no. 14, pp. 4470–4475, 2007.
- [30] N. D. Alikakos, G. Fusco, and G. Karali, "Ostwald ripening in two dimensions - The rigorous derivation of the equations from the Mullins-Sekerka dynamics," *J. Differ. Equ.*, vol. 205, no. 1, pp. 1–49, 2004.
- [31] H. Ghayour, H. R. Rezaie, S. Mirdamadi, and A. A. Nourbakhsh, "The effect of seed layer thickness on alignment and morphology of ZnO nanorods," *Vacuum*, vol. 86, no. 1, pp. 101–105, 2011.
- [32] L. E. Greene, M. Law, D. H. Tan, M. Montano, J. Goldberger, G. Somorjai, and P. Yang, "General route to vertical ZnO nanowire arrays using textured ZnO seeds,"

Nano Lett., vol. 5, no. 7, pp. 1231–1236, 2005.

- [33] N. T. Kemp, J. W. Cochrane, and R. Newbury, “Characteristics of the nucleation and growth of template-free polyaniline nanowires and fibrils,” *Synth. Met.*, vol. 159, no. 5–6, pp. 435–444, 2009.
- [34] N. T. Kemp, R. Newbury, J. W. Cochrane, and E. Dujardin, “Electronic transport in conducting polymer nanowire array devices.,” *Nanotechnology*, vol. 22, no. 10, p. 105202, 2011.

ACCEPTED MANUSCRIPT

Highlights

- Presence of crystallites affects memristor device performance.
- New method of reducing crystallites in microwave-assisted ZnO nanorod thin-films
- Heating rate is a significant contributor to the formation of large crystallites
- Control of the initial growth is essential for crystallite free ZnO nanorod films

ACCEPTED MANUSCRIPT